

Mechanical stabilisation of sacral bone injuries

L. Lobovský^a, M. Marešová^b, T. Mandys^a, M. Salášek^c, D. Weisová^c,
J. Krystek^b, J. Křen^{a,b}

^a*NTIS – New Technologies for the Information Society, Faculty of Applied Sciences, University of West Bohemia,
Univerzitní 8, 301 00 Plzeň, Czech Republic*

^b*Department of Mechanics, Faculty of Applied Sciences, University of West Bohemia, Univerzitní 8, 301 00 Plzeň, Czech Republic*

^c*Clinic for Orthopaedics and Traumatology of Locomotive Organs, University Hospital, alej Svobody 80, 323 00 Plzeň, Czech Republic*

In order to perform a thorough analysis of mechanical stabilisation of unstable pelvic ring injuries and to suggest their optimal treatment, a computational model based on finite element method is designed and verified using experimental data. Sacral bone fractures and especially the fractures with spinopelvic dissociation are of interest. Several osteosynthesis techniques for internal fixation of dorsal pelvis injuries are investigated. An attention is paid to minimally invasive osteosynthesis which employs transiliac internal fixation (TIFI) [3, 7], iliosacral screws (ISS) [1, 4] or lumbo-sacral fixations [5].

The conducted experimental study focuses solely on mechanical response of physical models of male pelvis with/without fracture and its treatment. These include models made of homogeneous isotropic material with linear mechanical response [8] as well as models with composite sandwich structure [9]. The latter mimics mechanical properties of real pelvic bones. On contrary to cadaveric pelvises, experiments with physical models provide repeatable data and their execution and control is substantially simplified. Mechanical properties of materials, the physical models are made of, are unambiguously determined.

The experimental pelvic tests are designed so that the uncertainty in the measured data is minimal. The models are tested under a quasi-static loading in craniocaudal direction while no displacements nor rotations in acetabula are allowed. Displacements and deformations of the pelvic bones are assessed using digital image correlation [6].

The applied experimental approach enables straightforward development of the computational model which precisely reflects the performed experiments. The geometry of the computational model is derived from the computed tomography scans of the physical models. The computational problem of elastostatics is solved and a surface-to-surface contact algorithm with a finite sliding formulation is employed between the fractured bone parts. Motion of all fixator screws within the bone tissue is fully constrained. In both computations and experiments, the effect of soft tissue structures is not reflected.

The computational model is verified for experiments on pelvic ring with either unilateral linear or unilateral comminuted fracture. Absolute displacements of the loaded sacral base, relative motion of the fractured bone parts and a symmetry of bone deformations are used as a key indicator of structural stability of the tested pelvis. In order to quantify the stability of each fixation technique, the stiffness ratio between the treated and the intact pelvic structure is introduced.

The verified computational model of pelvic ring is extended so that it includes the last two lumbar vertebrae and intervertebral discs. This enables modelling of lumbo-sacral fixation tech-

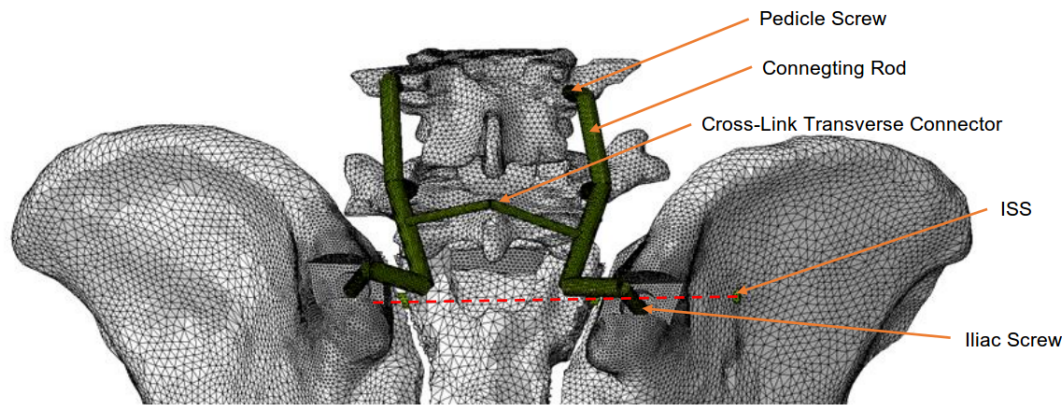


Fig. 1. Computational model of male pelvis with last two lumbar vertebrae and lumbo-sacral fixation

niques which provide superior results for unstable fractures with spinopelvic dissociation. In these cases, a lumbo-sacral fixation with a cross-link connector [2] is advantageous, Fig. 1. However, such technique requires an open surgery. This may be avoided when the cross-link connector is superseded by the ISS. The absence of the cross-link connector allows for a minimally invasive approach while the combination of the lumbo-sacral fixation with the ISS significantly increases stability of the treated pelvic structure.

Acknowledgement

This publication was supported by the European Regional Development Fund-Project "Application of Modern Technologies in Medicine and Industry" No. CZ.02.1.01/0.0/0.0/17_048/0007280.

References

- [1] Berber, O., Amis, A. A., Day, A. C., Biomechanical testing of a concept of posterior pelvic reconstruction in rotationally and vertically unstable fractures, *The Journal of Bone and Joint Surgery. British volume* 93-B (2) (2011) 237-244.
- [2] Cornaz, F., Widmer, J., Snedeker, J. G., Spirig, J. M., Farshad, M., Cross-links in posterior pedicle screw-rod instrumentation of the spine: A systematic review on mechanical, biomechanical, numerical and clinical studies, *European Spine Journal* (30) (2021) 34-49.
- [3] Dienstknecht, T., Berner, A., Lenich, A., Zellner, J., Mueller, M., Nerlich, M., Fuechtmeier, B., Biomechanical analysis of transiliac internal fixator, *International Orthopaedics* 35 (12) (2011) 1863-1868.
- [4] Giráldez-Sánchez, M. A., Lázaro-González, A., Martínez-Reina, J., Serrano-Toledano, D., Navarro-Robles, A., Cano-Luis, P., Fragkakis, E. M., Giannoudis, P. V., Percutaneous iliosacral fixation in external rotational pelvic fractures. A biomechanical analysis, *Injury* 46 (2) (2015) 327-332.
- [5] Lindahl, J., Mäkinen, T. J., Koskinen, S. K., Söderlund, T., Factors associated with outcome of spinopelvic dissociation treated with lumbopelvic fixation, *Injury* (45) (2014) 1914-1920.
- [6] Sutton, M. A., Orteu, J. J., Schreier, H. W., *Image correlation for shape, motion and deformation measurements*, Springer Science+Business Media, New York, 2009.
- [7] Ueno, F. H., Pisani, M. J., Machado, A. N., Rodrigues, F. L., Fujiki, E. N., Biomechanical study of the sacroiliac fracture fixation with titanium rods and pedicle screws, *Acta Ortopédica Brasileira* 23 (3) (2015) 154-157.
- [8] <https://www.sawbones.com/full-male-pelvis-large-solid-foam-w-sacrum-1301.html>
- [9] <https://www.sawbones.com/full-pelvis-large-4th-generation-composite-pelvis-fused-w-4th-generation-epoxy.html>

Numerical simulations of finite compressor cascade in 2D and 3D

P. Louda^a

^a*Institute of Thermomechanics, Czech Academy of Sciences, Dolejškova 5, Praha 8, Czech Republic*

The recent research at Institute of Thermomechanics AS CR includes measurements of flow through a model of compressor cascade [4]. In the experiment, suction of fluid from inter-blade channels is applied using relatively large slots in both side walls, see Fig. 1. In order to understand better the effect of suction, corresponding numerical simulations are carried out which are the subject of present article. The 3D solution domain consists of inlet channel, test section, and part of settling chamber of the wind tunnel, see Fig. 1. The suction slots are vented into common chamber with discharge piping on both ends (see Fig. 1, where the chamber itself is omitted in CAD drawing). Moreover, solid plates are positioned in the wakes of outer blades. Only half of the symmetrical test section is considered in simulations. Even so, the computational domain has 1 inlet and 6 outlets. The net flow rate is not known from measurement, therefore the inlet conditions are prescribed in order to meet the target Mach number in front of the cascade. On the outlet, target Mach number behind the cascade and net suction flow rate is known. In 4 outlets, the flow rate is dynamically adjusted to target values. One possibility of flow rate boundary conditions is given by Jirásek [2]. Other approach tested is dynamically adjusting average static pressure according to the 1D Bernoulli equation. Both approaches lead to same results.

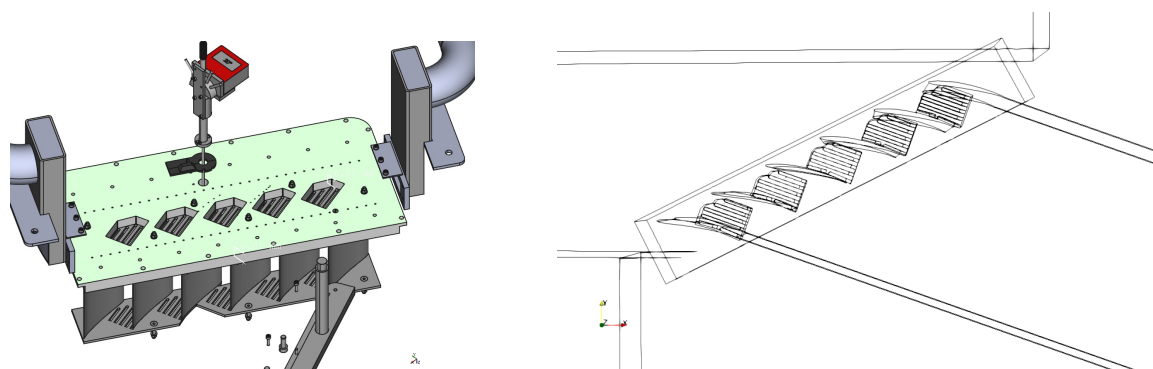


Fig. 1. Left: CAD model of the experimental cascade, right: corresponding computational domain

The mathematical model is based on Favre averaged Navier-Stokes equations for compressible flow. The turbulence is approximated by an explicit algebraic Reynolds stress model (EARSM) due to Wallin and Hellsten [1, 5].

The governing equations are discretized by an implicit finite volume method using hexahedral finite volumes in structured grid. Multi-block extension is used for complex geometry. The inviscid part of equations is approximated by the AUSMPW+ upwind method [3] with higher order interpolation in the direction of grid lines. The equations are linearized leading to block

7-diagonal algebraic system (if the boundary is neglected). The linear solver combines direct solver for 3-diagonal system with sweeps in other two directions. The implementation is in-house parallel code by the author. The grid is also generated by author's code and a zoom is shown in Fig. 2. The grid consists of approx. 5.5 mil. finite volumes in approx. 2000 blocks. The work to parallel processes is distributed block-wise.

The simulated regime corresponds to inlet Mach number 0.892, inlet angle of 61° and outlet Mach number 0.627 with outlet angle 45.6°. The isolines of Mach number in the cascade are shown in Fig. 3. One can see that there is large flow separation on 4th and 5th blade. This makes the simulation to some extent unsteady. The measurement corresponds to attached flow, however, differs somewhat in Mach number.

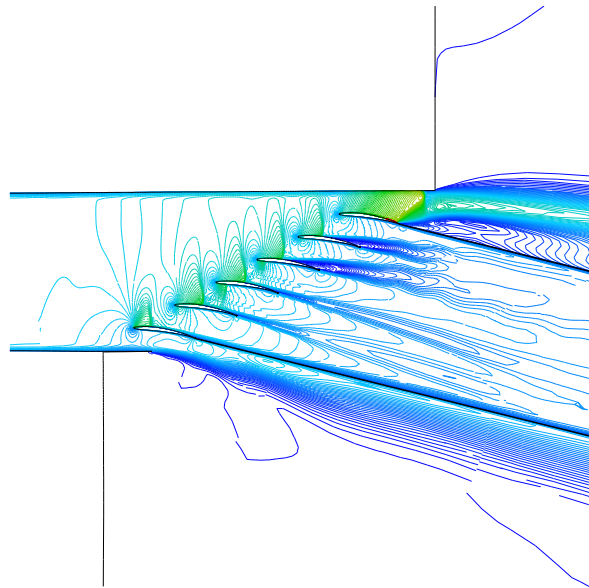
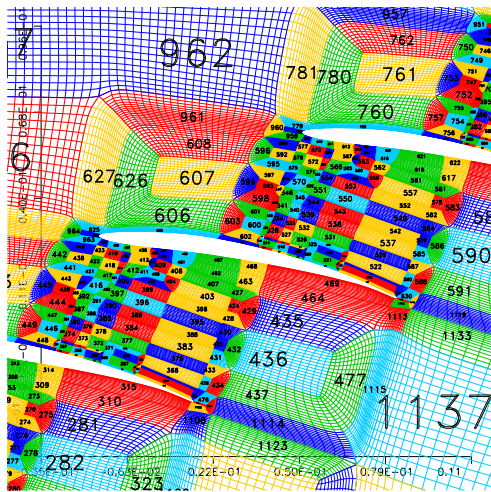


Fig. 2. Grid structure around the cascade

Fig. 3. Mach number isolines in the center-plane

The net influence of transversal flow can be expressed by means of the axial velocity density ration (AVDR) coefficient: $AVDR = \frac{(\int_0^t \rho_2 v_{ax2} ds)}{(\int_0^t \rho_1 v_{ax1} ds)}$, where subscript 1 denotes inlet and subscript 2 outlet. The AVDR for each inter-blade channel is shown in Table 1.

Table 1. AVDR coefficients for inter-blade channels

channel	simulation	measurement
1	1.261	
2	1.208	
3	1.154	1.178
4	0.774	
5	0.794	

The distribution of Mach number in the middle of suction slots is shown in Fig. 4. It should be noted that there is reverse flow near front and rear end of most slots. The line in the same figure denotes plane, which is shown in terms of Mach number in Fig. 5.

Simultaneously, 2D simulations are carried out, as well. They enable faster evaluation of inlet parameters since inlet is not much influenced by 3-dimensionality of the flow. To some extent, they could approximated flow in center-plane without suction. However, the 2D sim-

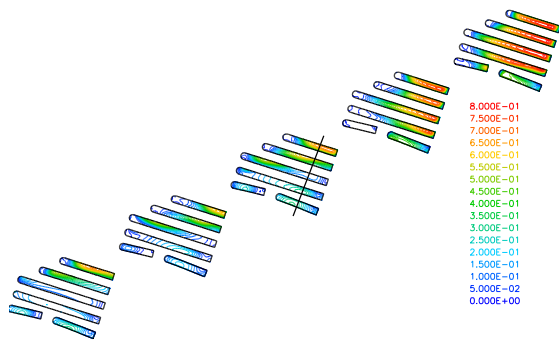


Fig. 4. Mach number in the suction slots

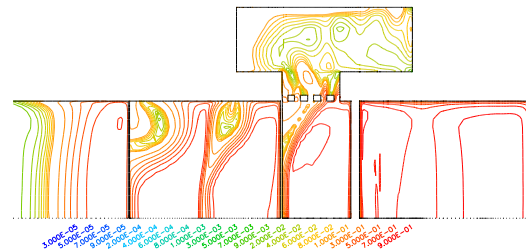


Fig. 5. Mach number of the secondary flow

ulation predicts some flow separation on all blades and it remains to be confirmed if it is the effect of suction from side walls.

As a preliminary conclusion, though, only 3D simulations probably can provide reliable results even if one considers the center-plane only. The convergence of numerical simulations is adversely affected by the need of dynamically adjusting flow rates in some outlets and by large overall dimensions of the solution domain compared to the cascade. Moreover, the parameters of flow regime in the experiment are found by trial and error. Nevertheless the simulation is the only way to visualize secondary flows in the present configuration.

Acknowledgment

The work has been supported by the project TK03030121 “Conceptual Design of an Innovative Safety System for Gas-cooled Nuclear Reactors” of the Technology Agency of the Czech Republic.

References

- [1] Hellsten, A., New advanced $k-\omega$ turbulence model for high-lift aerodynamics, *AIAA Journal* 43 (9) (2005) 1857-1869.
- [2] Jirásek, A., Mass flow boundary conditions for subsonic inflow and outflow boundary, *AIAA Journal* 44 (5) (2006) 939-947.
- [3] Kim, K. H., Kim, C., Rho, O.-H., Methods for accurate computations of hypersonic flows I. AUSMPW+ scheme, *Journal of Computational Physics* 174 (2001) 38-80.
- [4] Luxa, M., Šimurda, D., Measurements on compressor cascade KOBRA, Research Report Z 1649/21, Institute of Thermomechanics, Czech Academy of Science, v.v.i., 2022.
- [5] Wallin, S., Engineering turbulence modeling for CFD with a focus on explicit algebraic Reynolds stress models, Ph.D. thesis, Royal Institute of Technology, Stockholm, 2000.